SUPPORTING INFORMATION

Allosteric Activation of Metabotropic Glutamate Receptor 5

Balázs Jójárt, Zoltán Orgován, Árpád Márki, Gáspár Pándi-Szekeres, György G. Ferenczy and György M. Keserű*

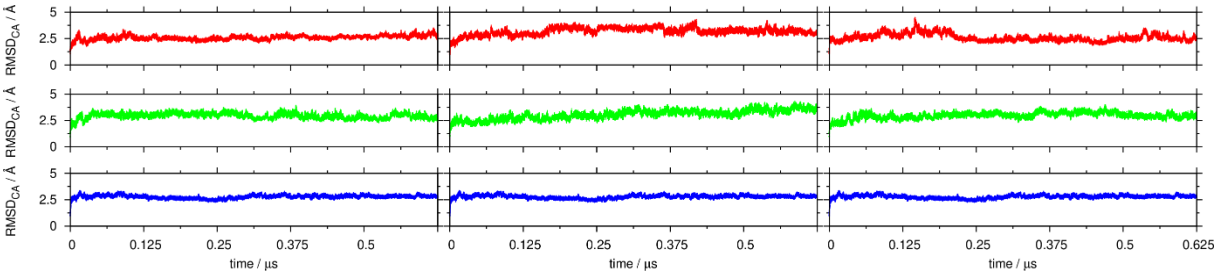

Figure S1. Cα RMSD for NAM (red), SAM (green) and PAM (blue) complexes in the MD simulations. Results for three simulations of each complex are shown. All values are in Ångströms

NPO			UPO	
Ile	621		Ser	654
Ile	625		Ser	658
Leu	627		Gln	704
Ile	651		Asn	747
Pro	655		Thr	781
Tyr	659		Ser	805
Val	740		Ser	809
Pro	743			
Leu	744			
Ile	751			
Ile	784			
Trp	785			
Phe	788			
Met	802			
Val	806			
Ala	810			
Ala	813			

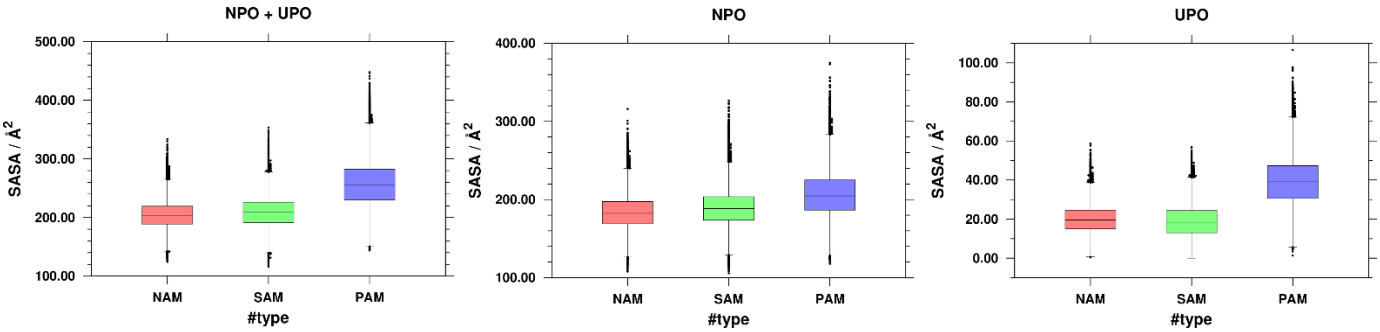

Figure S2. Solvent accessible surface area of the binding site with nonpolar (NPO), uncharged polar (UPO) and all (NPO+UPO) residues for the NAM (red), SAM (green) and PAM (blue) complexes. Residues within 4.5Å from the ligand during the whole MS trajectory were collected, and those present in over 1% of the trajectory were involved in the calculation and are listed.

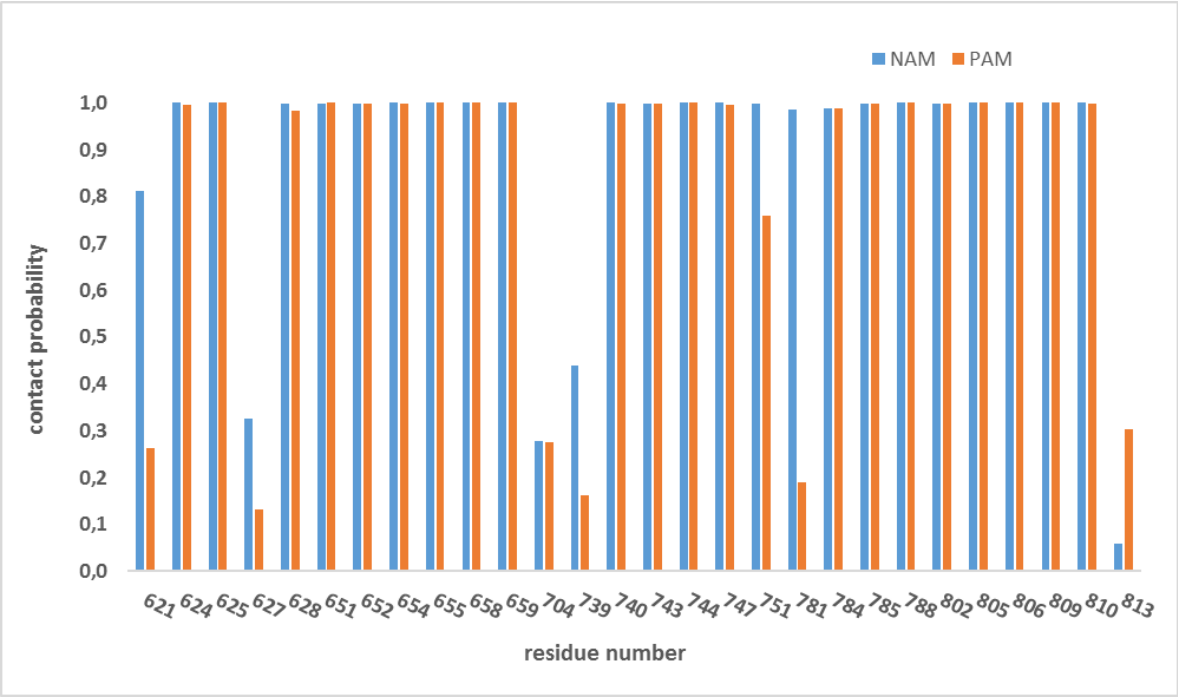

Figure S3. Ligand-protein contact probability for the NAM and PAM complexes applying 4.5Å distance cut-off. Residues with contact probability lower than 0.2 in both complexes are not shown. Contact probability was calculated as described by Deriu et al.(Deriu et al., 2014)

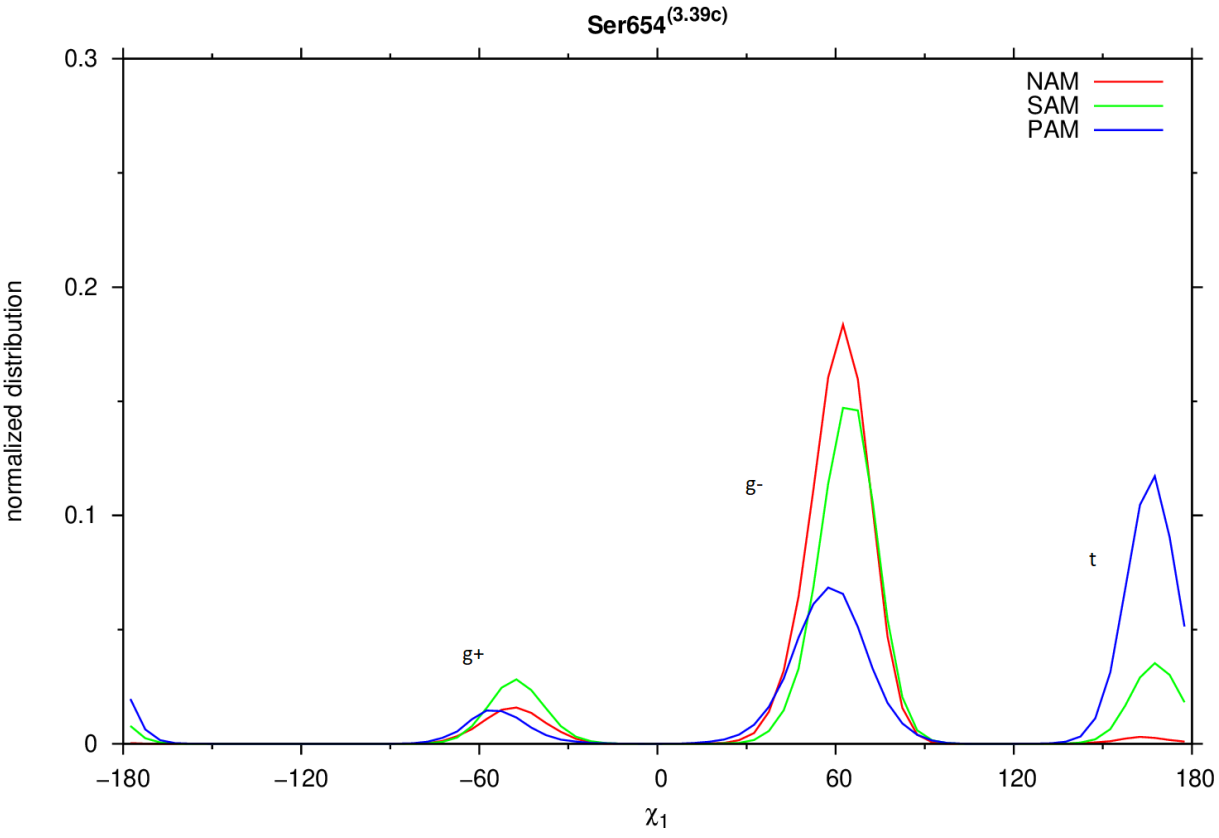

Figure S4. Distribution of S654$^{3.39c}$ side chain conformations in NAM (red), SAM (green) and PAM (blue) complexes.

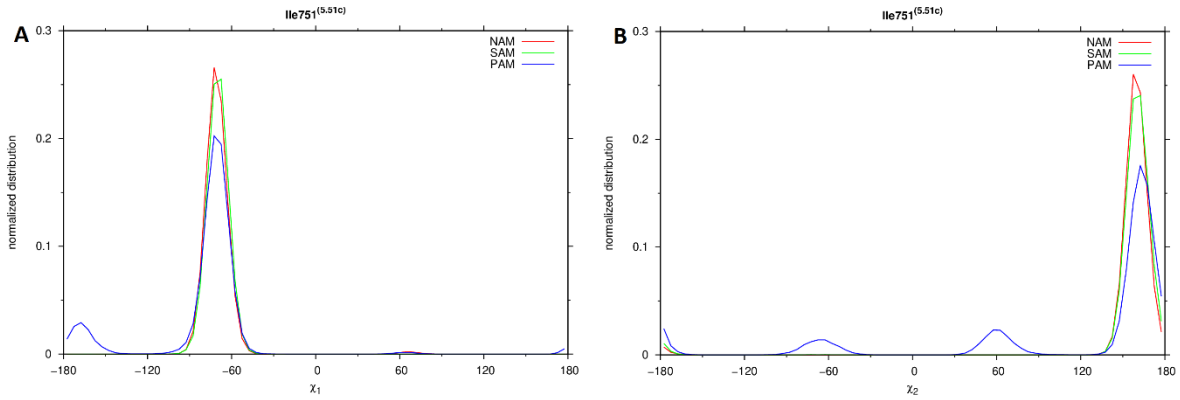

Figure S5. Distribution of Ile751$^{5.51c}$ side chain conformations in NAM (red), SAM (green) and PAM (blue) complexes. A) χ1(cα-cβ) B) χ2(cβ-cγ).

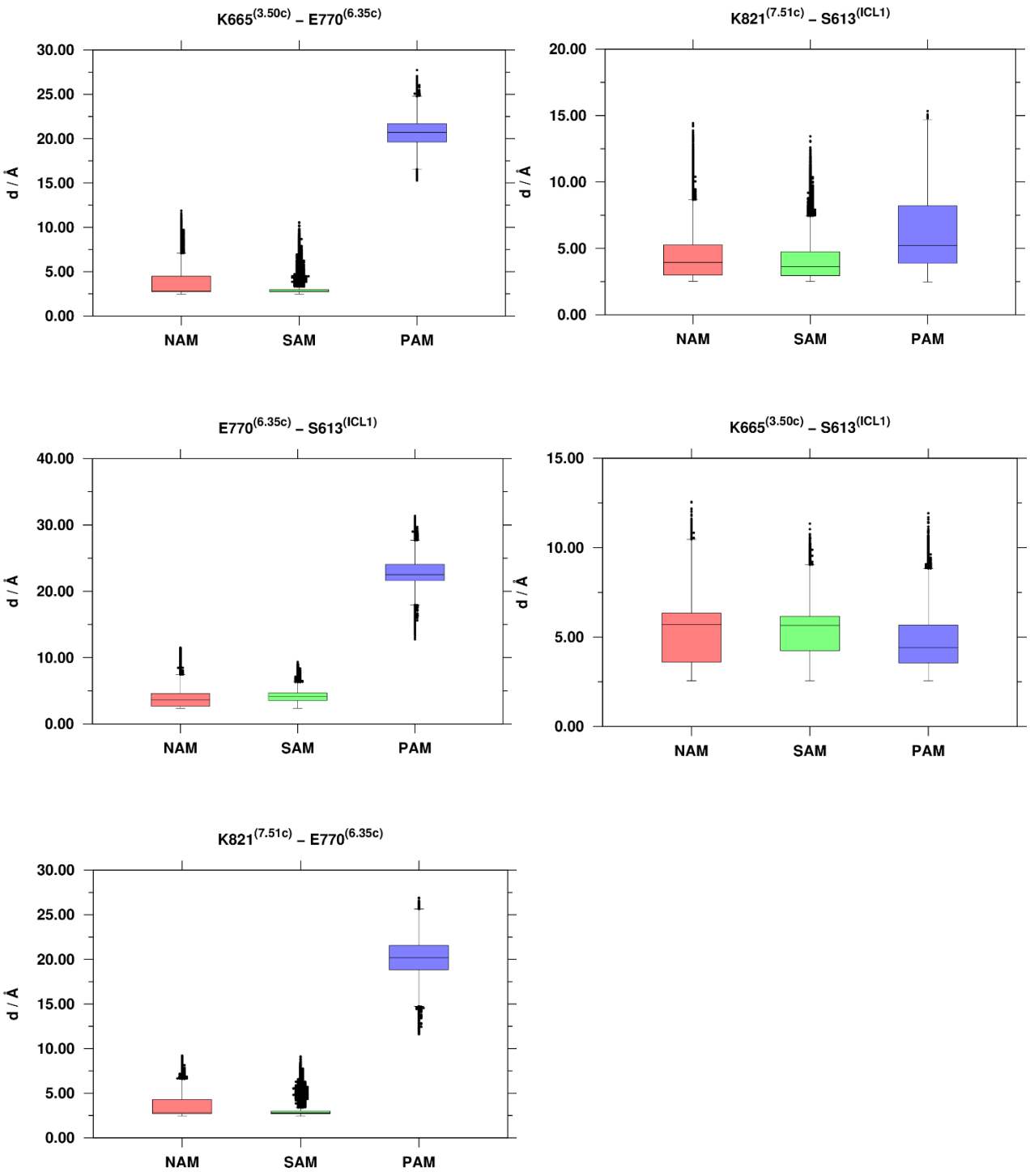

Figure S6. Distribution of distances between K665$^{3.50c}$, E770$^{6.35c}$, S613^{ICL1} and K821$^{7.51c}$. These residues form ionic and polar interactions in the NAM and SAM complexes fixing TM3, TM2, TM6 and TM7. The residues are separated by large distances in the PAM complex. red: NAM; green SAM; blue: PAM.

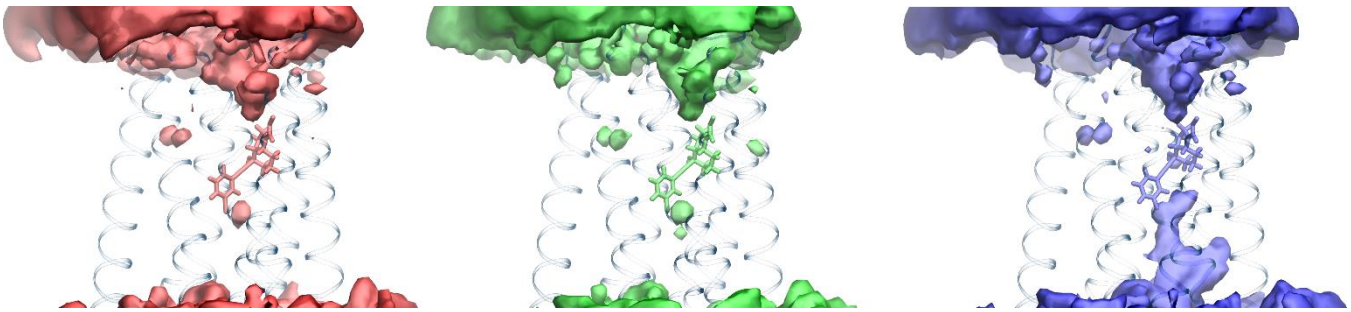

Figure S7. A continuous water channel is formed under the ligand at the intracellular side in the PAM complex (blue). This water channel was not observed in the NAM (red) and SAM complexes (green).

Table S1. RMSD of TM helices for the NAM vs. inactive X-ray structure (PDB: 4OO9) and PAM vs. active cryo-electron microscope structure (PDB: 6N51). Mean (stan. dev.) values are in Ångströms

Head 1[a]	NAM vs. 4OO9	PAM vs 6N51
TM1	0.89 (0.20)	1.70 (0.28)
TM2	0.72 (0.14)	1.31 (0.23)
TM3	0.99 (0.26)	2.65 (0.21)
TM4	0.84 (0.20)	2.35 (0.25)
TM5	0.71 (0.15)	1.82 (0.23)
TM6	0.96 (0.20)	2.62 (0.47)
TM7	0.94 (0.24)	1.67 (0.32)
all	0.90 (0.12)	2.12 (0.16)

Table S2. Number of water molecules in the 1st layer (R=3.4 Å) and 2nd layer (R=5 Å) of residues. Averages and standard deviations for the PAM and NAM complexes. Residues under the ligand toward the cytosolic region with the largest difference in neighboring water molecules in the PAM compared to the NAM complexes are shown.

PAM ID	PAM 1st_ave	PAM 1st_stdev	PAM 2nd_ave	PAM 2nd_stdev	NAM 1st_ave	NAM 1st_stdev	NAM 2nd_ave	NAM 2nd_stdev	diff_1	diff_2
ALA.771	7.42	1.92	15.83	3.76	3.41	1.10	5.72	1.72	4.00	10.11
THR.777	3.58	2.23	7.30	3.96	0.16	0.38	0.88	0.55	3.42	6.42
MET.778	3.29	2.31	6.41	3.48	0.06	0.25	0.71	0.53	3.23	5.70
LEU.662	3.78	2.28	7.81	3.67	0.65	0.68	1.74	1.08	3.13	6.07
THR.781	3.48	2.08	5.58	3.15	0.79	0.42	0.80	0.44	2.69	4.78
ILE.774	4.19	1.88	8.60	2.60	2.15	1.36	5.25	1.85	2.04	3.35
CYS.816	2.57	1.77	5.44	3.24	0.56	0.62	1.64	1.43	2.01	3.81

References

Deriu, M. A., Grasso, G., Licandro, G., Danani, A., Gallo, D., Tuszynski, J. A., & Morbiducci, U. (2014). Investigation of the Josephin Domain Protein-Protein Interaction by Molecular Dynamics. *PLoS ONE*, *9*(9), e108677. https://doi.org/10.1371/journal.pone.0108677